Research Article
Open Access
CrossMark

Turbulent flow velocity profiles downstream of an airfoil at different angles of attack (α)

Abstract

This investigation studied the influence of the angle of attack (α) on the turbulent flow behavior downstream of a NACA0015 airfoil installed in a subsonic wind tunnel. Velocity profiles were determined using a Prandtl tube, and a smoke flow visualization technique was used to visualize wake formation on a Clark Y airfoil. The results indicated that the average velocity decreases by 33% when the airfoil's angle of attack changes from 0° to 12°. Furthermore, it was found that at α=12°, a flow instability section occurs, generating a wake that occupies approximately 40% of the total velocity profile area.

Keywords: velocity profile, airfoil profile, angle of attack, wind tunnel, wake, smoke flow visualization

Volume 9 Issue 4 - 2025

Paz Mauricio Leonel, Morales Oscar Adrián, Paz Juan Antonio, Magaña Tonatiuh, Reyes Priscila Alexandra, Aguirre Alexis Erubiel
Autonomous University of Baja California, Tijuana, Mexico

Correspondence: Oscar Adrián Morales, Faculty of Engineering and Technology, Mechanical and Aerospace Engineering Program, Autonomous University of Baja California, Tijuana, Mexico, Tel +52 664 979 7591

Received: November 19, 2025 | **Published:** December 26, 2025

Abbreviation: NACA, national advisory committee for aeronautics; AOA, angle of attack

Introduction

In the work described by Rubel et al.,[1] conducted for the Bangladesh Army University of Science & Technology and Rajshahi University of Engineering & Technology in Bangladesh, the NACA0015 airfoil was studied at various angles of attack (AOA) for different airspeeds to determine the lift and drag force at each 2° angle of attack (α), from 0° to 18°. This experiment was performed in the low-speed wind tunnel of the Bangladesh Army University of Science & Technology, and a numerical analysis was also carried out using ANSYS®.[2] The wind tunnel in question has a cross-section of 0.3 m x 0.3 m and a length of 0.4 m, with an average speed in the test area of 8 to 10 m/s, as shown in the following Figure 1.

Figure 1 Wind tunnel of the Bangladesh Army University.

Rubel et al.,[1] designed and built the NACA0015 type airfoil and machined it at the University as shown in Figure 2, and also developed a mechanism that allows the angle of attack of the airfoil to be varied once mounted in the wind tunnel test area.

Figure 2 NACA 0015 airfoil and angle of attack variation mechanism constructed by Rubel et al.,[1]

The drag (CD) and lift (CL) coefficients shown in equation 1 were measured with a balanced arm (articulated mechanism) and the air speed was determined by an inclined tube manometer.

$$C_D = \frac{2F_D}{\rho u^2 A} \qquad (1)$$

$$C_L = \frac{2F_L}{\rho u^2 A}$$

For the numerical analysis, the computational domain is established from the tail edge to the inlet and outlet 12.5L (L=chord length), V4=H3=R5=12.5L. For the numerical analysis, it was necessary to add a fine mesh (15000 elements) to adequately model the flow field as shown in Figure 3. The boundary conditions established in the simulation are shown in the following Table 1:

Table 1 Boundary conditions for analysis by Rubel et al.,[1]

Input Parameter	Magnitude	Input Parameter	Magnitude
Solver type	Density based	AOA	0°–8°
Time	Steady	Kinematic viscosity	1.46E-05
Velocity of flow	8.5–9.65 m/s	Reynolds number	Varies with air velocity
Operating temperature	300 K	Number of iteration	1500
Operating pressure	1 atm	Angle of Attack	0°–18°
Viscous model	Laminar	Solution method	Second order upwind
Density of fluid (Ideal air)	1.23 kg/m³	Length	0.06 m

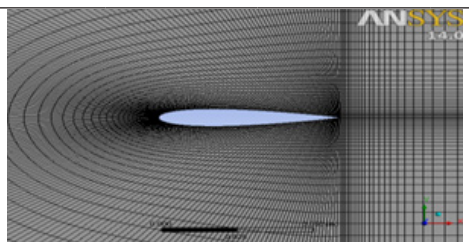

Figure 3 NACA 0015 airfoil mesh generated by Rubel et al.,[1]

Figure 4 shows the static pressure contours obtained in the numerical simulation by Rubel et al.,[1] and shows that it increases on the lower surface of the airfoil as the angle of attack increases, reaching a maximum value (61.4Pa) when the angle of attack is 12º.

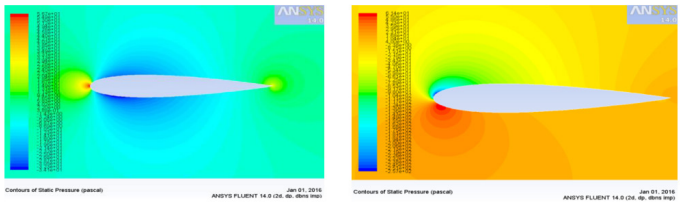

Figure 4 Pressure contours on airfoil at 0° (left) and 12° (right) angle of attack.

Figure 5 shows the velocity contours and reveals that the leading edge of the NACA0015 experiences a greater static force than the trailing edge. It is clear that the speed on the upper surface is greater than on the lower surface of the airfoil. A lower speed on the lower surface generates more lift.

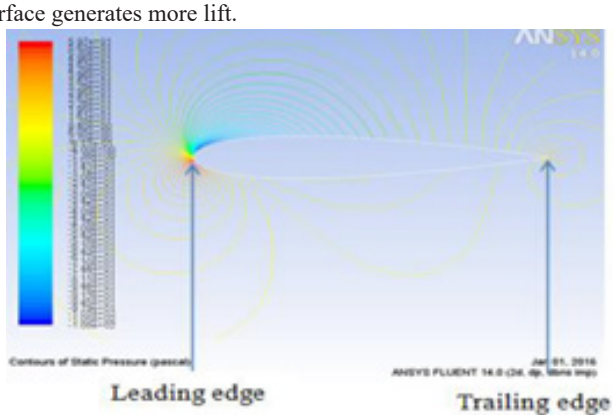

Figure 5 Speed contours with a 6° angle of attack.

Figure 6 shows the correlation curve of the coefficients obtained numerically and experimentally. It can be observed that the lift coefficient (CL) increases with increasing angle of attack up to a certain limit (0.22) and decreases after 12°. The drag coefficient (CD) increases with increasing angle of attack up to a maximum value of 0.07 at α = 18°. Finally, a maximum difference of 5% was found between the numerically and experimentally obtained results for the lift coefficient and 2% for the drag coefficient.

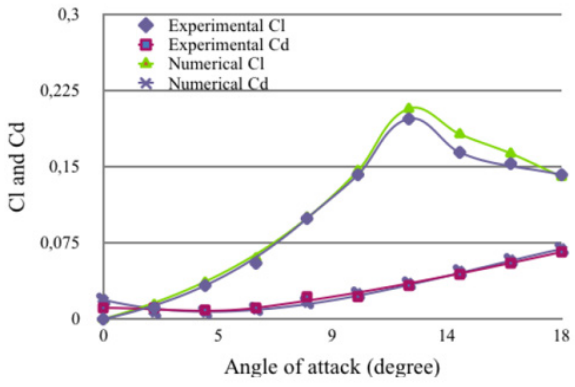

Figure 6 Variation of CL and CD with respect to the angle of attack (α).

Another study that addresses the analysis of lift and drag coefficients is the one proposed by Prudhvi.,[2] conducted for the Mahatma Gandhi Institute of Technology in Hyderabad, India. The coefficients were obtained using computational fluid dynamics (CFD) for a NACA 0015 airfoil. The justification for this approach, they state, is that using a wind tunnel is more expensive and laborious than analytical modeling. The angles of attack (α) analyzed were 0° and 6°. CATIA® software was used to model the three-dimensional computational domain shown in Figure 7a, and ANSYS® was used for meshing and solving the simulation. Figure 7b shows the finer meshing near the model. The boundary conditions are described in the following Table 2.

Table 2 Boundary conditions for Prudhvi analysis.[2]

No	Input	Value
1	Velocity of flow	0.15 Mach or 51 m/s
2	Operating temperature	300 K
3	Operating pressure	101325 Pa
4	Model	Transition SST (4th equation)
5	Density of fluid	1.225 kg/m³
6	Kinematic viscosity	1.4607×10^{-5}
7	Reynolds number	3.5×10^{6}
8	Length	1 m
9	AOA	0° and 6° respectively
10	Fluid	Air as an ideal fluid

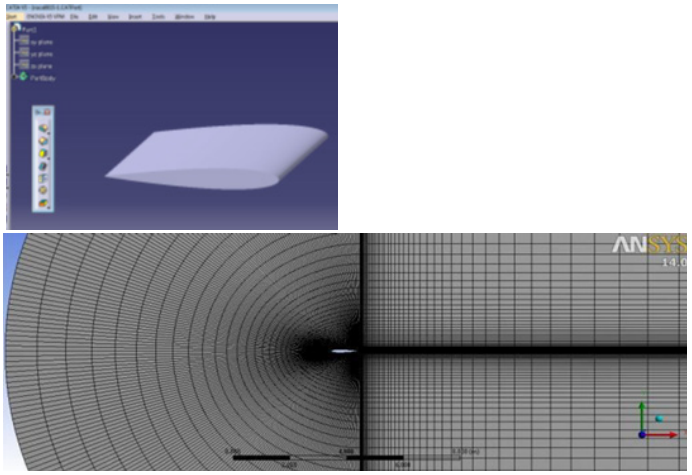

Figure 7 A) NACA 0015 airfoil profile in 3D, B) Fine mesh near the profile generated by Prudhvi.,[2]

The pressure contours observed are shown in Figure 8. It can be seen that for an angle of attack of 0°, these contours are symmetrical for the upper and lower sections, and the stagnation point is located exactly at the tip of the airfoil. Therefore, no pressure difference is generated between the two surfaces of the airfoil. On the other hand, for an angle of attack of 6°, we observe that the flow has a stagnation point just below the leading edge, which produces lift, since there is a low-pressure region on the upper surface of the airfoil. We can also observe that Bernoulli's principle is fulfilled: the velocity is high (indicated by the red contours) in the low-pressure region and vice versa. There is a high-pressure region at the leading edge (stagnation point) and a low-pressure region on the upper surface of the airfoil.

Regarding the velocity contours shown in Figure 9, at an angle of attack (AOA) of 0°, the velocity curves are symmetrical, and at an AOA of 6°, the stagnation point shifts slightly towards the trailing edge across the lower surface. This creates a low-speed region on the lower part of the airfoil and a higher-speed acceleration region on the upper part.

Citation: Leonel PM, Adrián MO, Antonio PJ, et al. Turbulent flow velocity profiles downstream of an airfoil at different angles of attack (α). *Aeron Aero Open Access J.* 2025;9(4):219–227. DOI: 10.15406/aaoaj.2025.09.00240

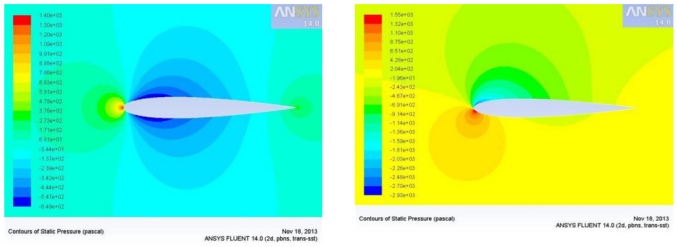

Figure 8 Pressure contours on airfoil at 0° (left) and 6° (right) angle of attack.

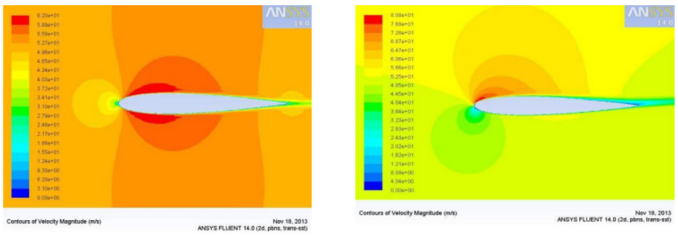

Figure 9 Velocity contours on NACA 0015 airfoil profile with AOA 0° (left) and 6° (right).

According to Bernoulli's principle, the upper surface will experience low pressure and the lower surface, higher pressure. Therefore, the lift coefficient will increase, as will the drag coefficient, but the increase in drag is small compared to the increase in lift. In a symmetrical airfoil with no incidence, the velocity distribution, and therefore the pressures, across both surfaces would have been exactly equal, canceling each other out and resulting in a net lift of zero.

Prudhvi.,[2] concludes that at zero angle of attack, no lift is generated, and if an increase in lift and lift coefficient is desired, the angle of attack (AOA) must be increased. In doing so, drag and drag coefficient obviously also increase, but the increase in drag and drag coefficient is considerably smaller compared to the increase in lift. The exact numerical values for the forces and coefficient are shown below (Table 3).

Table 3 Results of coefficients obtained by Prudhvi.,[2]

Variables	0 degree of AOA	6 degree of AOA
Drag force (N)	21.79	40.0502
Lift force (N)	0.2487	888.7298
Drag coefficient	0.01373	0.02566
Lift coefficient	0.00015	0.56947

A third investigation related to lift and drag coefficients in a NACA 0015 airfoil was conducted by Dhawale.,[3] for Walchand College of Engineering in Maharashtra, India. They performed a two-dimensional analysis using the commercial software ANSYS® Fluent. The angles of attack analyzed were 0°, 5°, 10°, and 15°. The fine meshing conditions used are presented in Table 4 and Figure 10. At the system inlet, the velocity was defined with an angle of attack of 0 degrees. The gauge pressure at the inlet was 0. At the outlet, the gauge pressure was also assumed to be 0. The airfoil surface was treated as a wall.

Table 4 Meshing conditions for dhawale analysis.[3]

Object Name	Surface Body
State	Meshed
Graphics Properties	
Visible	Yes
Transparency	1
Definition	
Suppressed	No
Coordinate System	Default Coordinate System
Thickness	1 m
Thickness Mode	Refresh on Update
Behavior	None
Reference Frame	Lagrangian
Material	
Fluid/Solid	Defined By Geometry (Solid)
Bounding Box	
Length X	25 m
Length Y	25 m
Properties	
Volume	557.83 m³
Centroid X	2.1769 m
Centroid Y	−1.6445e−008 m
Centroid Z	0 m
Surface Area (approx.)	557.83 m²
Statistics	
Nodes	60600
Elements	60000
Mesh Metric	None

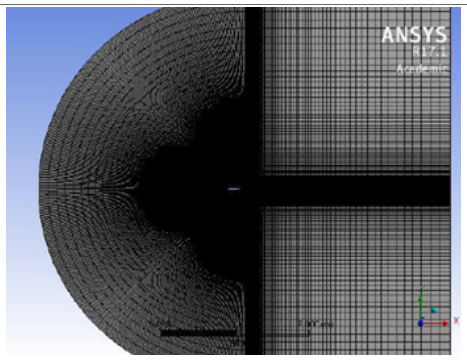

Figure 10 Fine mesh near the profile generated by Dhawale.,[3]

Figure 11 shows the pressure contours, and it was found that with zero lift, the pressure distribution on the upper and lower surfaces is identical. A static pressure contour shows that pressure increases on the lower surface of the airfoil as the angle of attack increases. In the absence of incidence, in the case of a symmetric airfoil, the velocity distribution, and therefore the pressure, along both surfaces would have been exactly the same, canceling each other out, and the total lift force would be zero.

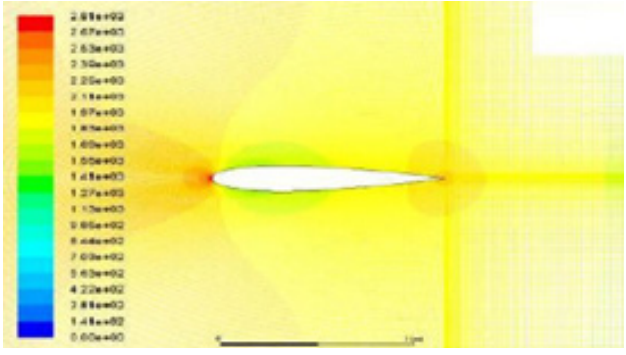

Figure 11 Pressure contours on NACA 0015 airfoil profile at 0°.

Citation: Leonel PM, Adrián MO, Antonio PJ, et al. Turbulent flow velocity profiles downstream of an airfoil at different angles of attack (α). *Aeron Aero Open Access J.* 2025;9(4):219–227. DOI: 10.15406/aaoaj.2025.09.00240

The results obtained for the lift and drag coefficients are presented in Table 5 and show that the lift coefficient varies with the angle of attack. A larger angle of attack is associated with a higher lift coefficient. After reaching the maximum lift coefficient, it decreases with increasing angle of attack. A symmetrical wing has zero lift at an angle of attack of 0°. Similarly, the drag coefficient is zero at an angle of attack of zero and increases slowly until stall. The critical or stall angle of attack is typically around 15° for many airfoils.

Table 5 Results of coefficients obtained by Dhawale.[3]

Theoretical			Calculated		Error %	
α	Cl	Cd	Cl	Cd	Cl	Cd
0	0	0.0156	0.0002	0.01818	–	16.55769
5	0.5483	–	0.53917	0.04063	-1.66514	–
10	1.0966	–	1.0286	0.06364	-6.20098	–
15	1.6449	–	1.6835	0.04845	2.346647	–
16	–	–	1.7714	0.05145	–	–

The table shows that the numerically obtained results are not far from the theoretically calculated results, with a low percentage of error. In conclusion, it is proposed that both coefficients increase in tandem with the angle of attack.

Another study that deals with a two-dimensional numerical analysis of the lift coefficient for different types of airfoils in the NACA series was carried out by Gonzalez et al.,[4] for the University of Cordoba in Colombia. The airfoils selected for the analysis were NACA 0015, NACA 0018, NACA 0021, and NACA 0025, due to the established conditions of availability for vertical-axis wind turbines and economic considerations. The airfoil coordinates were taken from the UIUC Applied Aerodynamics Group database.[5]

The boundary conditions used in the modeling were: a wall-type airfoil, two inlet velocities (one for the semicircle and one for the horizontal sides), and a pressure outlet for the rear vertical lines. The mesh quality in each mesh was verified using the skewness and orthogonal quality parameters. Figure 12 shows the fine mesh near the aerodynamic model.

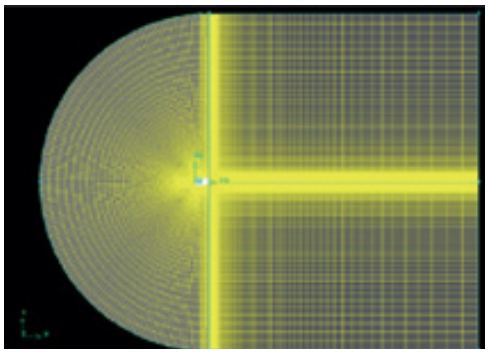

Figure 12 Fine mesh near the profile generated by Gonzalez et al.,[4]

For the solution, Gonzalez et al.,[4] used the K – ω SST (2eqn) simulation model, given its robustness at low Reynolds numbers, its formulation for the viscous layer, and its primary characteristic: a gradual transition from the standard K – ω model near the wall, with the ability to predict high Reynolds number behavior (K – ε) in the region outside the boundary layer. This model is widely used in aerospace and turbomachinery research.

The inlet conditions used were: subsonic Reynolds number of 1.6 x 10^5, free-stream temperature of 300 K, air density ρ = 1.225 kg/m^3, viscosity μ = 1.7604 x 10^{-5} kg/ms, and incompressible flow. The simulations were performed for angles of attack (α) between 0° and 30°.

To validate their numerical methodology, Gonzalez et al.,[4] compared the lift coefficient obtained for the NACA0025 airfoil with the information available in the SANDIA database. The difference found was 5.35%, which allows them to consider the process acceptable. Figure 13 shows the lift coefficient results as a function of α for the four airfoils evaluated. It can be observed that the lift coefficient for all airfoils at angles less than 15° has a similar behavior with values close to each other. For angles greater than 15°, the NACA 0015 airfoil presented a lift coefficient of 0.79 but is the airfoil with the greatest dynamic stall after 17°. The NACA 0018 had the highest lift coefficient value of 0.83; however, it exhibited a dynamic stall beyond 23°. The NACA 0021 airfoil presented a lift coefficient of 0.78 and a dynamic stall at approximately 20°. The NACA 0025 airfoil exhibited a lift coefficient of 0.71, the lowest value among the evaluated airfoils. However, it did not suffer dynamic stall, ensuring continuous operation because the lift forces did not fluctuate, resulting in greater blade stability due to the reduction of vibrations caused by lift stalls. Although the lift coefficient of the NACA 0025 airfoil is the lowest of all, it is very close to the values presented by the other airfoils.

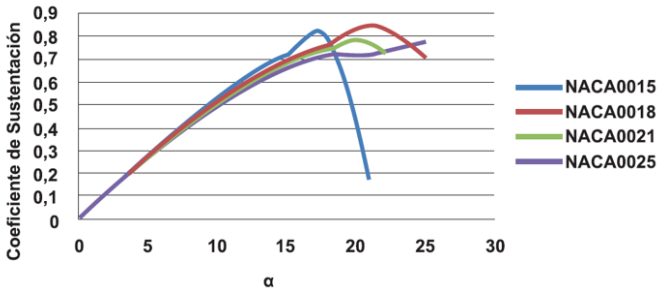

Figure 13 Variation of CL with respect to the angle of attack (α) for Re=160000.

Finally, Gonzalez et al.,[4] indicate that they selected the NACA0025 airfoil for the wind turbine they were designing because it exhibits a stable variation in the lift coefficient as a function of the angle of attack and a good drag/lift ratio among the airfoils evaluated. The dynamic stability and performance of this airfoil for the Re used in the simulations allows it to operate at wind speeds between 2 and 6 m/s, making it an ideal airfoil for low-power generation needs in H-type wind turbines.

A final reviewed study related to the flow around an airfoil profile is the one carried out by Arranz[6] in his undergraduate thesis for the Higher Technical School of Industrial Engineering (ETSII) of thePolytechnic University of Cartagena, Spain. The difference between this work and the previously presented research is that it analyzes turbulent flow around a NACA4412 airfoil at different angles of attack (0° to 16°) in a subsonic wind tunnel. The test area has a cross-section of 400 mm x 400 mm and a length of 1000 mm. The model, pressure measurement probes, and smoke injection probes are placed in this section, as shown in the following Figure 14.

Weather conditions are monitored using a weather station whose characteristics are: accuracy for temperature of 0.1ºC, for humidity 1% and for pressure is unknown.To determine the speed in the test area, a Pitot tube was used, and its measurements were applied in the following equation:

$$U = \sqrt{\frac{2 \cdot \rho_{agua} \cdot g \cdot \Delta h}{\rho_{aire}}} \quad (2)$$

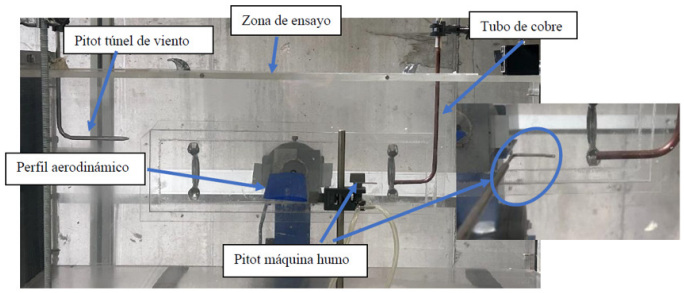

Figure 14 Subsonic wind tunnel test area of the ETSII.

Where: U is the average speed (m/s), is the density (kg/m3), g is gravity (9.81 m/s2) and Δh is the height difference of the inclined manometer (m).

The visualization technique used by Arranz,[6] it is the injection of smoke, and Figure 15a shows the generator used (Boomtone machine F400) and its arrangement during the experiment. The test area is illuminated using a green diode laser as shown in Figure 15b. The laser characteristics are: a wavelength of 532nm, output power of 50Mw, voltage of 3-5VDC, line thickness of 2mm to 1mm, and dimensions of 18mm x 75mm.

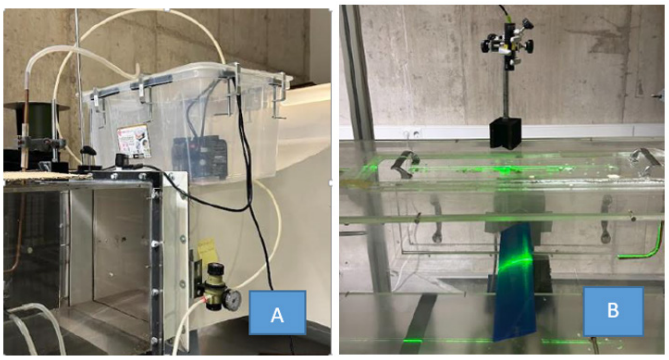

Figure 15 A) Smoke generator and injector machine

B) lighting of the test area.

The iPhone 14® mobile device camera was used for video recording and image capture. For video recording in the laboratory environment, a 4K recording setting at 30 frames per second (fps) was used, as this configuration provided the best video quality under laboratory conditions. Figure 16 shows the flow visualization over the NACA4412 airfoil with α=0º. It can be seen that the boundary layer is fully adhered to the airfoil. Figure 17 shows the flow over the airfoil with α=8º. It can be observed that boundary layer separation begins at the trailing edge. Figure 18 shows the flow over the airfoil with α=16º, and it is evident that the separation zone is increasing. It can be stated that the boundary layer is completely separated from the airfoil, since the low-pressure zone occupies practically the entire area of the airfoil.

Figure 19 shows the flow separation point more clearly. The pink area represents the detached boundary layer region, characterized by turbulent flow and increased vorticity, which can lead to velocity recirculation. This, in turn, generates a high-pressure zone. In contrast, the uncolored leading edge corresponds to a low-pressure region. The line separating these two areas is known as the parting line.

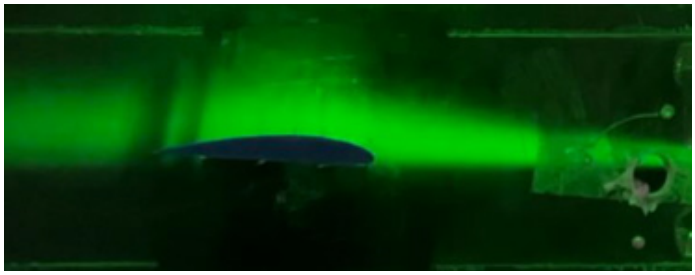

Figure 16 Flow over NACA 4412 profile with α =0°.

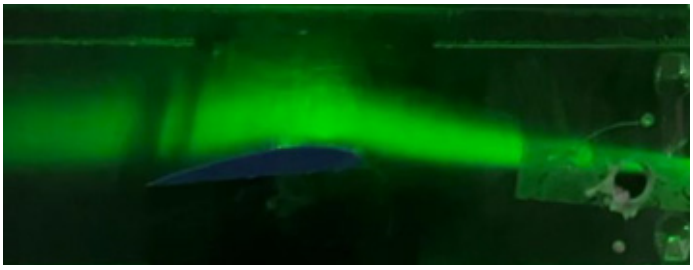

Figure 17 Flow over NACA 4412 profile with α =8°.

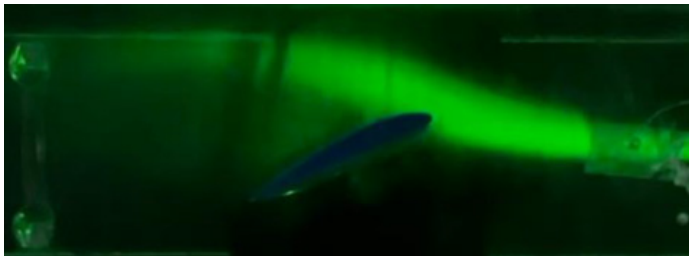

Figure 18 Flow over NACA 4412 profile with α =16°.

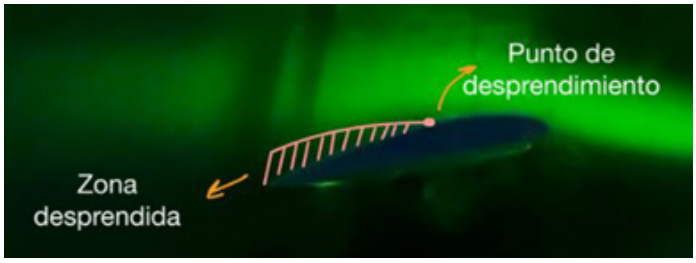

Figure 19 Representation of the separation and boundary layer in the NACA4412 airfoil profile.

When attention is focused on the separation line, it can be observed that as the angle of attack increases, the separation point moves upwards towards the leading edge.

It is schematically represented as follows (Figure 20):

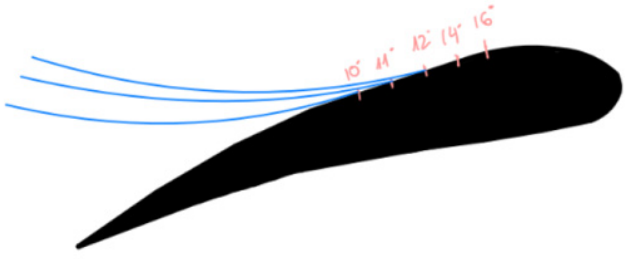

Figure 20 Schematic of the Arranz boundary layer detachment.[6]

Citation: Leonel PM, Adrián MO, Antonio PJ, et al. Turbulent flow velocity profiles downstream of an airfoil at different angles of attack (α). *Aeron Aero Open Access J.* 2025;9(4):219–227. DOI: 10.15406/aaoaj.2025.09.00240

But to demonstrate this phenomenon more clearly, a graph is made from the images taken, relating the percentage of detachment in terms of the rope and the angle of attack (Figure 21):

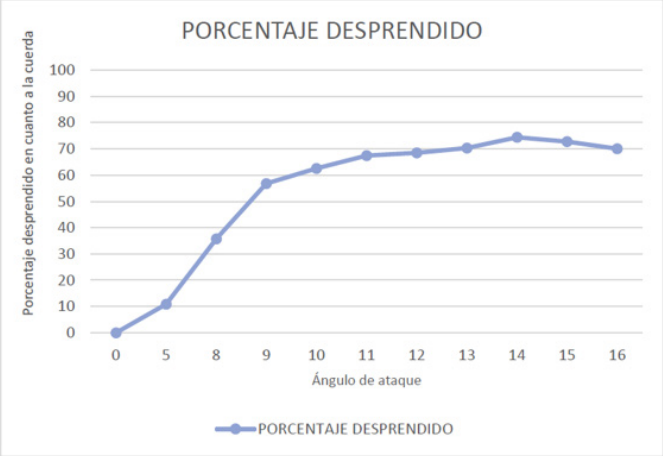

Figure 21 Displacement of the separation point with the angle of attack.

The author points out that the results obtained are approximate, as the values were derived from image measurements, but they allow for a graphical demonstration of the conclusions drawn from the images. It is confirmed that detachment begins when α=8º and the boundary layer is practically detached at α=14º, where the highest percentage of detachment along the chord is obtained, at approximately 80%.

Finally, the author compares her results with those obtained in the Bachelor's Thesis by Conesa,[7] noting that, although the Reynolds number was not the same, the results will be similar. Figure 22 shows the relationship between the angle of attack and the lift coefficient obtained by Conesa.[7] Of all the curves presented, attention should be focused on the blue line, as it represents the laboratory conditions. Total boundary layer separation corresponds to the point at which the lift value drops completely. However, as has been concluded, boundary layer separation is a gradual phenomenon.

The author states the following regarding this comparison:

a) Applying visualization techniques, it is concluded that detachment occurs within a range of 8 to 14 degrees.

b) In experimental results, it is concluded that detachment occurs in the range of 8 to 13 degrees.

As expected, the results are similar, but not completely identical. This can be explained by the following reasons:

a) Under the conditions in which I work Conesa [7] there is a higher Reynolds number, and as the flow speed increases with a lower angle of attack, total separation of the boundary layer will occur.

b) Among the drawbacks of visualization techniques are their lower precision and the possibility of a greater margin of error, since the results depend on what is observed by the human eye and its subsequent interpretation.

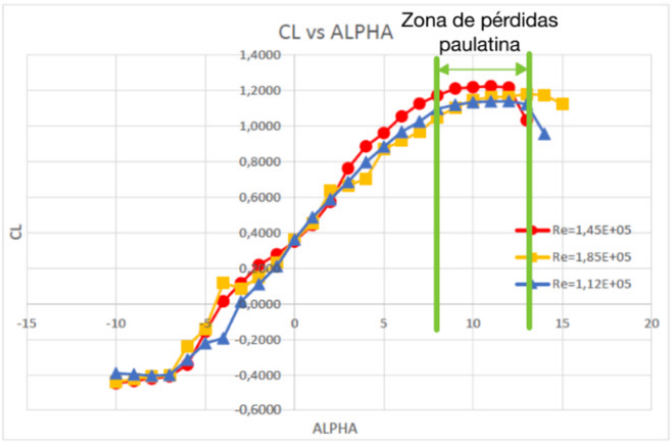

Figure 22 Lift coefficientobtained by Conesa.[7]

The reviewed research reveals ample information on the lift and drag coefficients of a NACA airfoil, specifically the 0015 series. However, the downstream airflow behavior and its relationship to the angle of attack are relatively unexplored areas of research. Therefore, this study focuses on analyzing the downstream airflow of the NACA0015 airfoil.

Experimental methodology

In the C15-10 subsonic wind tunnel,[8] the downstream velocity profiles of a NACA0015 type airfoil were analyzed with two different turbulent flow regimes and 3 angles of attack, as specified below (Table 6):

Table 6 Experimental matrix

Angle attack (α)	Reynolds number as a function of string length	Phenomenon analyzed	
		Speed profile	Flux trail
0° 6th 12th	Airfoil NACA0015 Re = 115866 Re = 129481	Measuring instrument: Prandtl tube.	Measuring instrument: Static pressure brush.
15°	Clark Y wing profile Re = 150328	----------	Visualization with smoke

The wind tunnel test area has a section of 0.150 m x 0.150 m x 0.455 m, and in this the symmetrical wing profile NACA0015 is placed, whose manufacturer's geometric specifications are chord of 0.615m and thickness of 9.2mm.

To determine the velocity profile downstream of the airfoil, a Prandtl tube is placed approximately 1 cm behind the NACA0015 as shown in Figure 23, and to determine the static pressure behavior in the flow wake, the measuring instrument called the static pressure brush shown in Figure 24 is placed in the same location as the Prandtl tube.

Citation: Leonel PM, Adrián MO, Antonio PJ, et al. Turbulent flow velocity profiles downstream of an airfoil at different angles of attack (α). *Aeron Aero Open Access J.* 2025;9(4):219–227. DOI: 10.15406/aaoaj.2025.09.00240

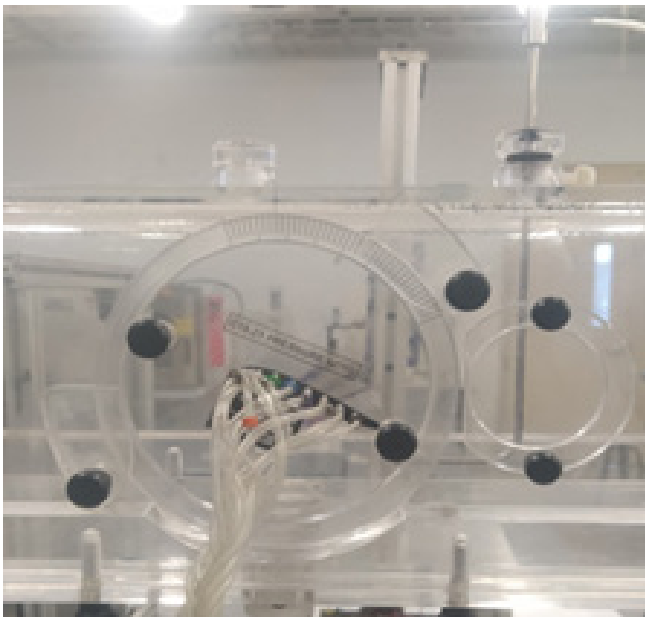

Figure 23 Prandtl tube in test area after the NACA 0015 airfoil profile.

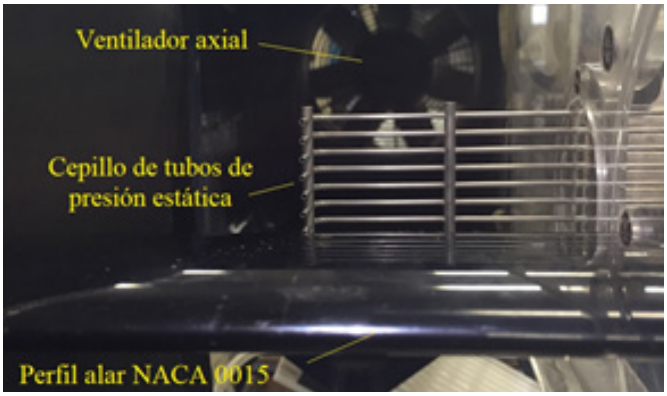

Figure 24 Static pressure brush immersed in the test area.

To characterize the test zone, the methodology indicated by Morales et al.,[9] is used, where the average air speed without any obstacle in the wind tunnel is determined as shown in Figure 25, the result indicates that the minimum average air speed is 29.57 ± 1.98 m/s and the maximum average speed has a magnitude of 33.04 ± 1.87 m/s, which corresponds to a turbulent regime.

Figure 25 Characterization of the test area.

To hold/fix the Prandtl tube in the test area, the utility model registered with the IMPI called Bushing for Pitot or Prandtl type pressure probe designed by Morales et al.,[10] is used, and to record all the pressure difference measurements made, the Extech brand digital anemometer model HD350[11] shown in Figure 26a is used, which is connected by USB cable to a computer in which the program included by the instrument is installed as shown in Figure 26b.

Figure 26 A) Extech brand digital anemometer

B) program installed on laptop computer.

Figure 27 shows the distribution of instruments in the test area for measuring the velocity profile downstream of the NACA 0015 airfoil. The velocity profile is determined along the Y axis by placing the Prandtl tube at 48 points, with the majority of them centered in the central section.

Figure 27 Installation of measuring instruments in the test area.

Experimental results

To calculate the average speed in all measurements, the air density value determined with the methodology indicated by CENAM is used,[12] the values used for its estimation are census andrecorded by the mini weather station developed by Morales et al.,[13] for FCITEC. The result obtained for the density during the characterization of the test area and its uncertainty was (Table 7):

Table 7 Air density and uncertainty

Magnitude	Worth	Units
Air density	1.140197	kg/m³
Uncertainty	0.092643	kg/m³

The average airspeed values obtained in the test area without the model inside and with the airfoil installed at different angles of attack are presented in the following table (Table 8):

Table 8 Test area characterization results

Fan power	Average speed (m/s)			
	Without wing profile	Wing profile α = 0°	Wing profile α = 6°	Wing profile α = 12°
80%	29.57 ± 1.98	28.49 ± 1.95	27.05 ± 1.82	19.24 ± 1.13
100%	33.04 ± 1.87	31.99 ± 1.86	30.03 ± 1.70	21.83 ± 1.09

The quantitative analysis of the results shown in Table 8 indicates, firstly, that the flow is turbulent in the test zone for both fan power levels used, with Reynolds numbers of 313705 for the maximum and 280758 for the minimum. It should be noted that these values are obtained when the test zone is unobstructed, so the Reynolds number is determined using the hydraulic radius of the test zone's cross-section. Based on these velocity and standard deviation measurements, the turbulence in this zone is estimated to be approximately 3%.

On the other hand, it is evident that the average velocity downstream of the NACA0015 airfoil reduces by approximately 33% when the airfoil's angle of attack changes from 0° to 12°. This is due to the wake generated by boundary layer separation in the central section of the duct downstream of the airfoil. To support this argument, a qualitative analysis is presented in Figure 28, which shows the visualization of turbulent flow over an airfoil at an angle of attack of 15° using the smoke technique described by Morales et al.[14] It can be seen that downstream of the airfoil, the smoke flow swirls in the wake zone, resulting in velocity vectors that flow in the opposite direction to the free-stream flow throughout this section. This flow recirculation phenomenon leads to a reduction in the average velocity downstream of the airfoil.

Figure 28 Flow wake in Clark Y airfoil profile.

The flow trail shown in the image corresponds to an ongoing investigation carried out in the FCITEC-01 wind tunnel on a Clark Y-type airfoil; however, the phenomenon is similar for a NACA0015-type airfoil, coinciding with what was reported in the investigation of Arranz[6] shown in Figure 19 and Figure 20.

The experimentally obtained velocity profiles for the two Reynolds regimes analyzed are presented in Figures 29 and 30. Both show the same flow behavior and a similar shape. The x-axis represents the relative velocity (u/umax), and the y-axis represents the position along this axis. Only the points are indicated; the coordinates for each are presented in the appendices. Some quantitative and qualitative aspects of each are detailed below.

At maximum and minimum fan power, the velocity profiles (blue lines in Figure 29 and Figure 30) for the test area without an aerodynamic model present a classic (logarithmic) shape of a turbulent flow, which represents a qualitative validation of the proposed result for the Reynolds numbers found. Furthermore, the shape obtained from the velocity profiles coincides with that published by Morales et al.1[5]

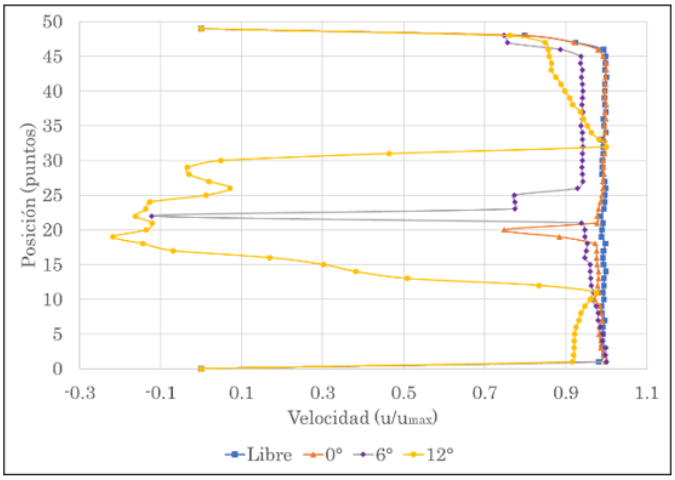

Figure 29 Speed profiles at minimum power of the wind tunnel fan.

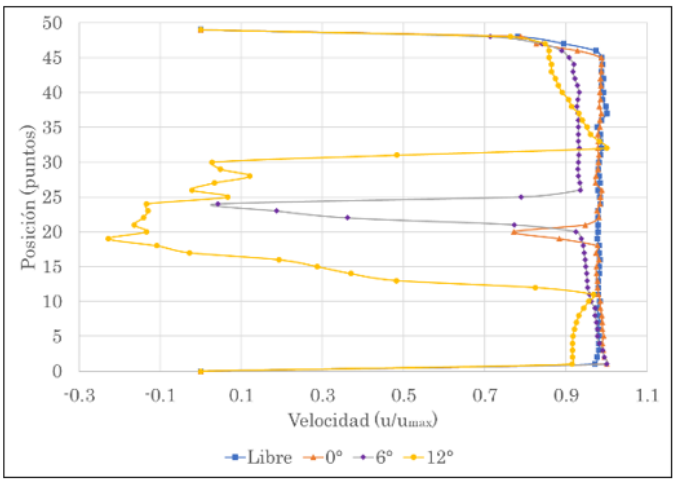

Figure 30 Speed profiles at maximum power of the wind tunnel fan.

At maximum and minimum fan power, the velocity profiles (yellow lines in Figure 29 and Figure 30) for the test area with the NACA0015 airfoil installed at an angle of attack of 12° show a larger flow instability section than the other two cases (α = 0° and 6°). There is a wake zone that occupies approximately 40% of the total airfoil section. This coincides with the findings of Rubel et al.,[1] Gonzalez.,[4] and Conesa.,[7] who observed that boundary layer separation occurs in a NACA-type airfoil at angles of attack greater than 8°. In the case where the airfoil has an angle of attack of α = 6°, the wake occupies 10% of the airfoil section, and in the case of α = 0°, the wake is barely perceptible.

Citation: Leonel PM, Adrián MO, Antonio PJ, et al. Turbulent flow velocity profiles downstream of an airfoil at different angles of attack (α). *Aeron Aero Open Access J.* 2025;9(4):219–227. DOI: 10.15406/aaoaj.2025.09.00240

As part of the quantitative analysis of the airflow behavior behind the NACA0015 airfoil and given that the case of an angle of attack at 12º is the most interesting to review, Table 9 presents the results of the measurement made with the static pressure brush, and it can be seen that in the central section there are the values of greater suction (negative pressure), which corresponds to the wake behavior as illustrated in Figure 28 and the airfoils shown above.

Table 9 Results of static pressure measurement in the wake

Fan power	Static pressure (Pa) with α = 12º									
	1	2	3	4	5	6	7	8	9	10
80%	-20	-235	-10	-39	-10	-29	-20	-29	-20	-137
100%	-29	-412	-20	-78	-20	-39	-29	-39	-39	-137

Conclusion

Experimental and numerical analysis of turbulent flow downstream of a NACA0015 airfoil profile was performed.

The maximum and minimum Reynolds numbers being studied are 129481 and 115866 respectively, based on the chord length of the wing profile. The average downstream speed of the NACA0015 airfoil is reduced by approximately 33% when the airfoil changes its angle of attack from 0° to 12°

For α=12º, a flow instability section occurs, reaching a wake that occupies approximately 40% of the total velocity profile section. The results are consistent with what has been reported in the literature, which states that at an angle of attack of 12º a wake is generated that leads to a collapse. The velocity profiles obtained numerically have a shape (qualitative result) similar to those found experimentally for both flow regimes.

Acknowledgements

None

Conflict of interest

Author has no conflicts of interest.

Funding

None.

References

1. Rubel R, Uddin K, Islam Z, et al. Numerical and experimental investigation of aerodynamics characteristics of NACA 0015 aerofoil. *Int J Eng Tech.* 2016;2(4):132–141.
2. Prudvhi K, Santosh K, Ajay S. CFD analysis of NACA 0015 aerofoil. *Int J Appl Innov Eng Manag.* 2018;7(3):1–7.
3. Dhawale S, More O, Gude R, et al. Computational fluid dynamic analysis of airfoil NACA 0015. *Int J Mech Eng Technol.* 2017;8(2):1–10.
4. Gonzalez D, Geovo C, Gonzalez D. Selection of the optimal symmetrical air profile for a vertical axis wind turbine using computational flow dynamics. *Rev Ingeniare.* 2017;13(22):83–91.
5. UIUC Applied Aerodynamics Group, Aerospace Department. Airfoil coordinates database.
6. Arranz C. *Visualization of the flow around an aerodynamic profile in a wind tunnel.* Thesis. Polytechnic University of Cartagena; 2023.
7. Conesa M. *Experimental and numerical study of the aerodynamic profile with NACA 4412 curvature.* Thesis. Polytechnic University of Cartagena; 2022.
8. Armfield Ltd. Armfield website. 2025.
9. Morales O, Gómez A, Paz J, Navarro J, et al. Characterization of the subsonic wind tunnel of ECITEC-UABC. *Rev Ingenierías.* 2018;21(80):6–20.
10. Morales OA, Paz JA, Gómez A. Bushing for Pitot or Prandtl tube type pressure probe. Utility model No. 5267. IMPI-Mexico. 2023.
11. Extech Instruments. Extech website. 2025.
12. Becerra S, Guardado G. *Estimation of uncertainty in the determination of air density.* National Metrology Center; 2003.
13. Morales OA, Paz JA, García A, et al. Mini weather station for wind tunnel. Utility model in process. File No. MX/f/2024/002997. IMPI-Mexico; September 30, 2024.
14. Morales O, Paz J, Gómez A, et al. Numerical-experimental analysis of the mixing capabilities of a porous medium in turbulent regime. In: *Proceedings of the XXVIII International Congress of SOMIM.* 2022:T1-T9.
15. Morales O, Gómez A, Vázquez R. Measurement of speed profiles in a wind tunnel. *Iberoam J Acad Prod Educ Manag.* 2014;2.